# Bond ionicity of the halogen–silver interaction

Paul S. Bagus, Gianfranco Pacchioni, and Michael R. Philpott

Citation: The Journal of Chemical Physics **90**, 4287 (1989); doi: 10.1063/1.455785
View online: http://dx.doi.org/10.1063/1.455785
View Table of Contents: http://scitation.aip.org/content/aip/journal/jcp/90/8?ver=pdfcov
Published by the AIP Publishing

# Bond ionicity of the halogen–silver interaction

Paul S. Bagus, Gianfranco Pacchioni,[a] and Michael R. Philpott
*IBM Research Division, Almaden Research Center, San Jose, California 95120-6099*

(Received 1 November 1988; accepted 21 December 1988)

The nature of the bonding between halogen atoms (F, Cl, and Br) and the Ag (111) surface has been investigated by analyzing *ab initio* Hartree–Fock wave functions for cluster models of the Ag surface and a halogen atom. Using a variety of criteria, we conclude that the bonding is ionic and that the halogen ionicity is essentially $-1$. The measures of ionicity reported are (a) the expectation value of a projection operator which provides an indication of the total charge associated with the halogen atom, (b) the analysis of the dipole moment curve as function of distance, (c) the effect on the equilibrium bond distances of a uniform external electric field, and (d) the decomposition of the interaction energy into the sum of different contributions. This latter analysis shows that the bonding arises, almost entirely, from two effects: (1) the Coulomb attraction between the charged halogen and the metal and (2) the intraunit polarization of the metal and halogen subunits.

## I. INTRODUCTION

The interaction of halogen atoms with Ag surfaces has been studied for well defined Ag(111) surfaces in ultrahigh vacuum, UHV, and on Ag electrodes in electrochemical environments. For Cl/Ag(111), Lamble *et al.*[1] have used surface extended x-ray absorption fine structure, SEXAFS, to determine the surface structure for 1/3 of a monolayer, ML, and 2/3-ML of Cl. For both coverages, they find that Cl is at a threefold site at a vertical distance of 4.13 a.u. above the Ag surface. In addition, *in situ* SEXAFS measurements of bromide adsorbed on Ag(111) electrodes at full coverage were recently performed and Ag–Br bond distances determined.[2] Adsorption of chloride, bromide, and iodide (fluoride does not contact adsorb from aqueous solutions because it is highly hydrated) on polycrystalline noble metal electrodes has been extensively studied.[3–7] In some cases both coverage and electrosorption valence (essentially charge on the adsorbed ion) were determined. However, there is little agreement on electrosorption valence perhaps due to differences in experimental method and conditions. The interpretation of these measurements to obtain the adsorbate ionicity requires several assumptions and detailed theoretical modeling of what happens as an ion approaches a surface would be very valuable.

The primary purpose of the cluster model studies described in this paper is to establish the nature of the bonding of halogen atoms, F, Cl, and Br, chemisorbed on a Ag(111) surface. We find the bonding is unequivocally established, through several different criteria, to be ionic; the adsorbate halogen carries essentially a charge of $-1$. The criteria for establishing the ionic character of the bonding have been developed in a series of recent papers.[8–10] These include: (1) Projection of the halogen character on the total cluster wave function; (2) Analysis of the dipole moment curve as a function of the distance of the halogen from the Ag surface; (3) Use of a constrained space orbital variation,[11] CSOV, analysis to separately characterize the importance of intraunit polarizations and interunit charge flow and covalent bonding; and (4) the effect of an applied external electric field on the equilibrium distance of the halogen from the surface. These criteria are not subject to the artifacts which arise from the more commonly used Mulliken population analysis.[12] Taken together, they give a consistent view and strong evidence for an ionic bond for all of the halogens considered, F, Cl, and Br.

In the following section, Sec. II, we describe the features of the cluster model and the molecular orbital, MO, wave functions. For all cases, we consider adsorption at the eclipsed, tetrahedral, threefold site of Ag(111). In Sec. III. we present the evidence given by all four criteria for the ionic character of the adsorbed halogen. In Sec. IV, we consider adsorption of F on clusters modeling the octahedral threefold hollow site of Ag(111). Finally in Sec. V, our conclusions are summarized.

## II. WAVE FUNCTION DETERMINATION

The $Ag_4X$ cluster, X = F,Cl,Br, is used to model the interaction of X with Ag at a threefold tetrahedral site of the Ag(111) surface; see Fig. 1. A threefold site for adsorption is reasonable and is supported by experimental data (see, e.g., Ref. 1). This cluster contains the nearest Ag neighbors of the halogen; these are the atoms that are most directly involved in the Ag–X bond. For the Ag atoms, an effective core potential (ECP)[13] has been used; the 28 electrons from the deep core 1*s* to 3*d* shells are represented by the ECP while the 19 electrons arising from the 4*s*, 4*p*, 4*d*, and 5*s* shells are explicitly included in the wave function. We call this operator a 19 electron ECP to distinguish it from an ECP which explicitly includes only the 11 Ag electrons from the 4*d* and 5*s* shells, an 11 electron ECP,[14] and from an ECP which includes only the outermost 5*s* electron, a 1 electron ECP.[15] The 11 and the 1 electron Ag ECP's have also been used, in particular for larger clusters, as will be discussed below. For the halogens, all electrons are included in the self-consistent field (SCF) cluster wave functions.

[a] Permanent address: Dipartimento di Chimica Inorganica e Metallorganica, Universita' di Milano, 20133 Milano, Italy.

 0021-9606/89/084287-09$02.10  

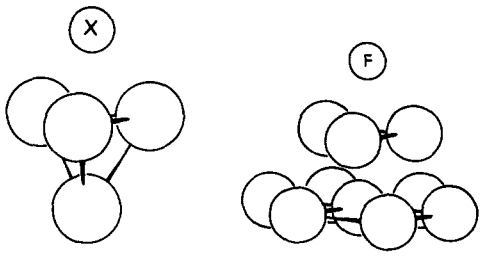


FIG. 1. Schematic representation of the $Ag_4(3,1)X$; X = F,Cl,Br, and of the $Ag_{10}(3,7)F$ clusters modeling the tetrahedral site on the Ag(111) surface. The halogen atom is above the center of the triangle formed by the three Ag surface atoms.

The molecular wave functions have been determined using flexible basis sets of contracted Gaussian-type orbitals, GTO's. The valence basis set for Ag has been contracted to 4*s*4*p*3*d*; see Ref. 13 for the GTO exponents and the ECP parameters. The basis sets for the halogen atoms, optimized for the neutral atoms,[16–18] were extended with diffuse *s*, *p*, and *d* functions whose exponents have been determined in order to obtain a better approximation for the SCF electron affinity[19] (EA) and for the dipole polarizability,[20] $\alpha_D$, of the anions. The neutral halogen basis sets are denoted as basic while the basis sets with the added functions are denoted extended. The halogen GTO basis sets, exponents, and contraction coefficients, are given in Table I. In Table II, the values of the halogen EA and $\alpha_D$ computed with the present basis sets are compared to Hartree–Fock limit values[19,20] and, for the EA's to experiment.[21] The computed EA values are very close to the Hartree–Fock limit values,[19] but differ substantially from the corresponding experimental ones (Table II). The lack of correlation effects is the main reason for this discrepancy.[22] For $\alpha_D$, our calculated values with the extended halogen basis sets are 25%–30% smaller than the Hartree–Fock limit.[20] However, they do reproduce the

TABLE I. Extended GTO basis set for halogen atoms.[a]

| | Fluorine | | Chlorine | | Bromine | |
|---|---|---|---|---|---|---|
| | Exp. | Coef. | Exp. | Coef. | Exp. | Coef. |
| *s* | 18 648.5 | 0.000 537 | 28 656.3 | 0.001 592 | 379 677.0 | 0.000 384 |
| | 2 790.77 | 0.004 160 | 4 299.00 | 0.012 202 | 56 125.1 | 0.003 000 |
| | 633.258 | 0.021 439 | 976.335 | 0.060 988 | 12 967.3 | 0.014 890 |
| | 178.599 | 0.083 438 | 274.415 | 0.213 429 | 3 836.08 | 0.054 774 |
| | 57.789 6 | 0.240 206 | 89.0063 | 0.453 700 | 1 331.99 | 0.156 771 |
| | 20.455 5 | 0.438 883 | 31.2371 | 0.396 630 | 508.042 | 0.332 810 |
| | . . . | . . . | . . . | . . . | . . . | . . . |
| | 7.587 96 | 1.0 | 31.2371 | 0.117 005 | 207.781 | 0.398 567 |
| | . . . | . . . | 7.769 51 | −0.354 30 | 90.421 8 | 0.176 530 |
| | 1.992 13 | 0.236 128 | 3.079 33 | −0.739 10 | . . . | . . . |
| | 0.749 854 | 0.597 574 | . . . | . . . | 33.004 3 | 1.0 |
| | . . . | . . . | 3.079 33 | 0.523 128 | 14.356 3 | 1.0 |
| | 0.241 845 | 1.0 | 0.651 038 | −1.265 8 | 4.728 52 | 1.0 |
| | 0.09 | 1.0 | . . . | . . . | 2.032 97 | 1.0 |
| | | | 0.240 798 | 1.0 | 0.412 706 | 1.0 |
| | | | 0.09 | 1.0 | 0.156 141 | 1.0 |
| | | | | | 0.03 | 1.0 |
| *p* | 63.125 3 | 0.008 563 | 150.436 | 0.028 503 | 3 167.91 | 0.002 464 |
| | 14.501 2 | 0.057 641 | 34.710 1 | 0.177 297 | 762.504 | 0.019 590 |
| | 4.382 33 | 0.200 680 | 10.407 1 | 0.480 085 | 249.396 | 0.091 169 |
| | 1.453 55 | 0.387 023 | 3.373 30 | 0.495 741 | 95.231 7 | 0.265 602 |
| | . . . | . . . | . . . | . . . | . . . | . . . |
| | 0.463 237 | 1.0 | 0.748 495 | 1.0 | 39.923 0 | 0.435 543 |
| | 0.126 578 | 1.0 | 0.207 855 | 1.0 | 17.781 6 | 0.311 776 |
| | 0.035 | 1.0 | 0.058 | 1.0 | . . . | . . . |
| | | | | | 7.677 26 | 0.351 228 |
| | | | | | 3.342 06 | 0.569 853 |
| | | | | | . . . | . . . |
| | | | | | 1.442 42 | 1.0 |
| | | | | | 0.442 320 | 1.0 |
| | | | | | 0.137 772 | 1.0 |
| | | | | | 0.03 | 1.0 |
| *d* | 0.12 | 1.0 | .67 | 1.0 | 96.150 0 | 0.026 513 |
| | | | .07 | 1.0 | 27.839 1 | 0.150 064 |
| | | | | | 9.851 06 | 0.380 489 |
| | | | | | . . . | . . . |
| | | | | | 3.610 18 | 0.480 277 |
| | | | | | 1.251 54 | 0.247 885 |
| | | | | | . . . | . . . |
| | | | | | 0.06 | 1.0 |

[a] The basic basis sets (see the text) are taken from Refs. 16–18; they do not contain the most diffuse *s*, *p*, and *d* functions.

TABLE II. Total energy ($E_T$) electron affinity (EA) and dipole polarizability ($\alpha_D$) values for halogen anions computed with basic and extended GTO basis sets.

| | $F^-$ | $Cl^-$ | $Br^-$ |
|---|---|---|---|
| $E_T(X^-)$ (a.u.) | | | |
| Extended | −99.438 19 | −459.314 00 | −2 572.162 64 |
| BSSE ($Ag_4$ extended)[a] | −99.438 85 | −459.319 54 | −2 572.164 45 |
| Hartree–Fock limit[b] | −99.459 37 | −459.576 70 | −2 572.535 50 |
| EA (eV) | | | |
| Basic | 1.37 | 1.65 | 2.09 |
| Extended | 1.35 | 2.08 | 2.52 |
| Hartree–Fock limit[b] | 1.36 | 2.58 | 2.58 |
| Experimental[c] | 3.40 | 3.62 | 3.36 |
| $\alpha_D$ (Å$^3$) | | | |
| Basic | 0.12 | 0.12 | 0.53 |
| Extended | 1.35 | 3.77 | 6.19 |
| BSSE ($Ag_4$ extended)[a] | 1.54 | 4.26 | 6.32 |
| Hartree–Fock limit[d] | 1.71 | 5.89 | 8.18 |

[a] The distance of the $Ag_4$ basis set from the halogen atom corresponds to halogen–Ag surface distances of 3.3, 4.3, and 4.8 a.u. for F, Cl, and Br, respectively.
[b] See Ref. 19.
[c] See Ref. 21.
[d] See Ref. 20.

large increase in $\alpha_D$ going from $F^-$ to $Cl^-$ to $Br^-$. If the basic halogen basis sets are used and the diffuse GTO's are not included, the $\alpha_D$'s are very small; see Table II.

For all clusters considered, the halogen atom to surface distance has been varied along the $C_{3v}$ axis to give potential energy and dipole moment curves.

It is possible for the $Ag_4X$ cluster calculations that the Ag atom basis functions may improve the description of the halogen atom properties. This may be true, in particular, for the $\alpha_D$ where, as we have shown, the values with the extended basis set differ by significant amounts from the Hartree–Fock limit values. This basis set superposition error, BSSE, may introduce artifacts in the analysis of the halogen–Ag interaction.[12] We estimate the BSSE by computing $\alpha_D$ for the halogen anions using the full basis set of the four Ag atoms in $Ag_4X$ as well as the halogen basis. The Ag basis sets are placed at the positions that the Ag atoms would have near the calculated equilibrium distance of the halogen from the $Ag_4$ cluster. With the ghost basis sets, we compute the BSSE $\alpha_D$ values from the change in the halogen anion energy due to a uniform electric field[23] $\Delta E = -1/2\alpha_D F^2$. The BSSE values for the extended halogen basis set are given in Table II. The BSSE leads to a modest improvement of the $\alpha_D$; we shall show later that the uncertainty of the analysis for the halogen–Ag interaction due to this BSSE is not large.

For distances close to the equilibrium Ag–halogen distance, the ground state configuration of $Ag_4X$ is $(1a_1)^2(2a_1)^2(3a_1)^2(1e)^4(2e)^1(^2E)$; the halogen cores as well as the Ag $1s^2$ to $4d^{10}$ cores are not given explicitly. This state arises from the combination of the $Ag_4$ ground state $(a_1)^2(e)^2$ with the seven valence *ns* and *np* electrons of X in configuration $(a_1)^2(a_1)^2(e)^3$. The main bonding effects are in the outer *e* shells and can be either covalent or ionic. In the latter case, the bonding can be considered as originating from the interaction of the ionized $Ag_4^+$ $(a_1)^2(e)^1$ cluster and the closed shell anion $X^-$ $(a_1)^2(a_1)^2(e)^4$. In the covalent view, a filled bonding $(1e)^4$ and a singly occupied antibonding $(2e)^1$ MO are formed.

Properties of the $Ag_4X$ interaction are given in Table III. These include the equilibrium distance of X above the Ag surface plane, $z_e$, the dipole moment at $z_e$, $\mu_e$, the vibrational frequency, $\omega_e$, the anharmonicity,[24] $\omega_e x_e$, and the dissociation energy, $D_e$. The $\omega_e$ and $\omega_e x_e$ are computed by matching a fourth degree polynomial expansion of the potential energy curve for the points on the curve near $z_e$. The $D_e$ is computed with respect to either dissociation to neutral units, $Ag_4$ and X, denoted $D_e(Ag_4 + X)$, or dissociation to ionic units, $Ag_4^+$ and $X^-$, denoted $D_e(Ag_4^+ + X^-)$. When a bond has a large degree of ionic character, Hartree–Fock values of $D_e$ with respect to neutrals may have a large error because the Hartree–Fock ionization potential, IP, and EA are not accurate. In this case, it has been shown[25] that $D_e$ with respect to the ionic limits corrected by experimental value for the IP and EA of the dissociation products gives quite accurate values for the $D_e$. It is worth noting that the computed bond distance for Cl on Ag(111), an Ag–Cl distance of 2.84 Å, is close to, but somewhat larger than, the value of 2.70 Å obtained from EXAFS measurements by Lamble *et al.*[1] Given the very shallow potential energy curve, small $\omega_e = 180\ cm^{-1}$, this is satisfactory agreement for an SCF calculation. It provides evidence for the adequacy of our cluster model.

TABLE III. Chemisorption properties for halogen atoms on $Ag_4$ and $Ag_{10}$ clusters.

| Cluster | | $Ag_4F$[a] | $Ag_4F$[b] | $Ag_{10}F$[c] | $Ag_4Cl$[a] | $Ag_4Br$[a] |
|---|---|---|---|---|---|---|
| $z_e$ | (a.u.) | 3.310 | 3.289 | 3.304 | 4.347 | 4.721 |
| $r_e$(Ag–X) | (Å) | 2.42 | 2.40 | 2.41 | 2.84 | 3.00 |
| $\mu_e$ | (a.u.) | −1.09 | −1.17 | −0.37 | −1.72 | −2.00 |
| $\omega_e$ | ($cm^{-1}$) | 277 | 273 | 255 | 180 | 115 |
| $\omega_e x_e$ | ($cm^{-1}$) | 0.8 | 0.8 | 0.9 | 0.4 | 0.2 |
| $D_e(Ag_n + X)$ | (eV) | 2.72 | 2.62 | 1.92 | 2.68 | 2.76 |
| $D_e(Ag_n^+ + X^-)$ | (eV) | 5.88 | 5.79 | 4.56 | 5.09 | 4.74 |

[a] All the Ag atoms are treated with a 19 electron ECP.
[b] All the Ag atoms are treated with a 11 electron ECP.
[c] The four Ag atoms defining the tetrahedral chemisorption site are treated with a 11 electron ECP; the neighboring Ag atoms are treated with a 1 electron ECP.

A major concern in cluster model studies is the dependence of the chemisorption properties on the size and shape of the cluster. In order to verify the generality of the results obtained with the small $Ag_4$, cluster we considered a second cluster model containing three Ag atoms in the first layer and seven Ag atoms in the second layer (Fig. 1); the cluster is used with a F adsorbate only. The total cluster is denoted $Ag_{10}$ (3,7)F or, simply, $Ag_{10}F$. In this case, the computational effort has been reduced by treating the four Ag atoms defining the tetrahedral chemisorption site with an 11 electron ECP in which the 4*s* and 4*p* electrons are not considered explicitly.[14] The six neighboring Ag atoms in the second layer have been treated with a 1 electron ECP[15] in which all the shells except the 5*s* are represented by an ECP.

The reliability of the Ag 11 electron ECP in studying halogen chemisorption has been tested comparing the results for $Ag_4F$ obtained with the two approaches, namely including the 4*s* and 4*p* electrons in the ECP or treating them explicitly. The results, reported in Table III, indicate a substantial agreement of the two sets of calculations. This guarantees that the use of the 11 electron ECP for the study of the larger $Ag_{10}$ cluster is possible without losing accuracy.

The bond distance and vibrational frequency determined for F on $Ag_{10}$ (Table III) are close to those obtained with the smaller $Ag_4$ cluster; on the other hand, the binding energy is about 25% smaller in the $Ag_{10}$ case. However, this result is not too surprising considering that oscillations in chemisorption energies usually occur varying the cluster size and shape, at least for relatively small clusters.[26] The slow convergence of $D_e$ to the experimental value is generally related to the character and energy of the cluster frontier orbitals. In the case of ionic interactions, the important substrate cluster properties are its effective work function and its polarizability. The important conclusion of the comparison of $Ag_4F$ with $Ag_{10}F$, as discussed in the following sections, is that the nature of the interaction is not dependent on the cluster nuclearity.

The 11 electron ECP has been used also for the investigation of $Ag_6$(3,3) and $Ag_7$(3,3,1) clusters interacting with F (Fig. 2). These two clusters model the octahedral threefold hollow site of the Ag (111) surface and allow a comparison of this site with the tetrahedral one represented by the $Ag_4$ cluster. The results for these two clusters are discussed in the last section.

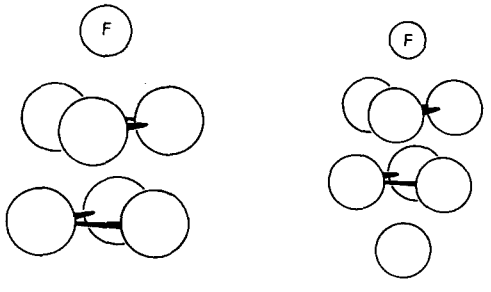


FIG. 2. Schematic representation of the $Ag_6$(3,3)F and of the $Ag_7$(3,3,1) clusters modeling the octahedral site on the Ag(111) surface. The halogen atom is above the center of the triangle formed by the three Ag surface atoms.

## III. EVIDENCE FOR BOND IONICITY IN Ag-HALOGEN INTERACTION

### A. Projection of halogen charcter in $Ag_4X$

A measure of the extent to which an orbital, $\varphi$, is occupied in a many-electron wave function, $\Psi$, is given by the expectation value, $P_\varphi$, of the projection operator, $P(\varphi)$,

$$P(\varphi) = \varphi\varphi^\dagger ,$$

$$P_\varphi = \langle \Psi | P(\varphi) | \Psi \rangle . \quad (1)$$

The details given about projection operators in Ref. 8 are summarized here. The value of $P_\varphi$ is not dependent on the basis set expansion used to construct $\Psi$; thus, projection avoids the artifacts often associated with population analysis.[8] The projected orbitals, $\varphi$, are chosen to have a well defined physical significance; in this paper, orbitals of the isolated adsorbate are used. If the $\varphi$ are taken to be the spatial parts of spin–orbitals and spatial degeneracy is neglected, then $P_\varphi \leqslant 2$. There are three cases for values for $P_\varphi$. In case I, $P_\varphi \approx 2$ and $\varphi$ is completely occupied in $\Psi$; in case II, $P_\varphi \approx 0$ and $\varphi$ is not occupied at all. These two limiting cases have the simplest interpretation. In the third case are the intermediate values, $0 < P_\varphi < 2$, giving an indication of a covalent bond. For the analysis of this case, it is necessary to take into account the overlap between the orbitals of the isolated adsorbate and substrate when these two subunits are superposed. To estimate the total charge on the halogen atom in $Ag_4X$, a sum over all the orbitals occupied in the isolated halogen anion is formed. The number of electrons given by this projection operator is denoted by $N_P$ and the effective charge associated with the halogen as $Q_P = Q_N - N_P$ where $Q_N$ is the nuclear charge.

For distances near $z_e$, values of $N_P$ and $Q_P$ are given in Table IV; the projections do not change significantly for large variations of $z$ about $z_e$. For all the halogens, F, Cl, and Br, the ionicity given by $Q_P$, is essentially $-1$. It is worth noting that no difference is found when the Ag surface is represented by the $Ag_4$ or $Ag_{10}$ clusters (Table IV). For all the individual halogen orbitals, case *I* or $P_\varphi \approx 2$ holds; all the halogen orbitals are fully occupied in $Ag_4X$. In other words, the projection gives strong evidence that $Ag_4X$ is properly described as $Ag_4^+$ and $X^-$. Although the projection indicates a deviation from the ionicity of $-1$ that is trivial for F, it does suggest that there might be a covalent contribution, albeit small, for Br; this is discussed further in Sec. III C, below.

### B. Dipole moment curves for $Ag_4X$ clusters

A commonly used way to estimate the ionicity of an adsorbate is based on the experimentally observed change in the work function, $\phi$, between a clean surface and an adsor-

TABLE IV. Projection of $X^-$ on $Ag_4X$ and $Ag_{10}F$ clusters.

| | $Ag_4F$ | $Ag_{10}F$ | $Ag_4Cl$ | $Ag_4Br$ |
|---|---|---|---|---|
| $N_P$ | 9.98 | 9.98 | 17.95 | 35.92 |
| $Q_P$ | −0.98 | −0.98 | −0.95 | −0.92 |

TABLE V. Taylor expansion of $\mu(z)$ for $Ag_nX$ and for localized $X^-$ orbitals in $Ag_nX$; see Eqs. (3) and (4). All $M_i$ are in a.u.

| | | $Ag_4F$ | $Ag_{10}F$ | $Ag_4Cl$ | $Ag_4Br$ |
|---|---|---|---|---|---|
| $\mu(Ag_nX)$ | $M_0$ | −1.09 | −0.37 | −1.72 | −2.00 |
| | $M_1$ | −1.39 | −1.50 | −1.60 | −1.59 |
| | $M_2$ | −0.09 | −0.27 | −0.04 | −0.01 |
| | $M_3$ | +0.01 | +0.07 | +0.03 | −0.03 |
| $\mu(X)$ | $M_0$ | −2.90 | −3.00 | −3.31 | −3.43 |
| | $M_1$ | −1.00 | −0.99 | −1.10 | −1.11 |
| | $M_2$ | +0.10 | −0.06 | −0.03 | −0.04 |
| | $M_3$ | −0.01 | +0.04 | +0.04 | −0.01 |

bate covered surface (see, e.g., Refs. 27–29 and references therein). This approach is used because the change in $\phi$ is due to a change in the surface dipole to which the redistribution of charge between substrate and adsorbate makes a significant contribution. In terms of the cluster properties of $Ag_4X$, an estimate obtained in this way, denoted $Q_D$, could be given by

$$Q_D \sim [\mu(Ag_4X) - \mu(Ag_4)]/z_e\,, \tag{2}$$

where $\mu(Ag_4X)$ is the cluster dipole for X at equilibrium, $z_e$, and $\mu(Ag_4) = -0.78$ a.u. is the dipole moment of the bare cluster. Equation (2) assumes that charge is taken from the surface layer of Ag and distributed spherically about the halogen; polarization effects are neglected. In Table V, Taylor expansions about $z = z_e$ are given for the dipole moment curve as a function of $z$;

$$\mu(Ag_4X;z) = M_0 + M_1(z - z_e) + M_2(z - z_e)^2 + M_3(z - z_e)^3 + \cdots; \tag{3}$$

the first term, $M_0$, is $\mu(Ag_4X;z_e)$. Using the values in Tables III and V, Eq. (2) leads to $Q_D(F) \sim -0.1$, $Q_D(Cl) \sim -0.2$, and $Q_D(Br) \sim -0.3$. These estimates are dramatically smaller than the $Q_D \approx -1$ given in Table IV; they suggest a covalent rather than ionic bond.

However, the linear behavior, small $M_2$ and $M_3$, which is found for all X, is consistent with an ionic bond[8] where the slope, $M_1$, is related to the extent of ionicity. The dipole moment of two point charges $+q$ and $-q$ will be $\mu = -q\times r$ and $d\mu/dr = -q$, assuming that $-q$ is at positive $r$ with respect to $+q$. Hence for an ideal fully ionic molecule where $q = 1$, $d\mu/dr = -1$ and the curve is a straight line. Unfortunately, it is possible to obtain two, quite different, estimates of the ionicity from the $M_1$ for $Ag_4X$. For the first, the polarization of both the $Ag_4$ and X subunits is neglected; then $Q = M_1$, where $Q$ is the effective charge of the halogen atom X. Since, for all X, the $|M_1|$ in Table V are larger than one, this estimate of $Q$ indicates that Rydberg levels in addition to the halogen rare gas cores are occupied; this is hardly likely. The second way of estimating the ionicity from $M_1$ arises from the use of image charge theory (see Ref. 29 and references therein) to describe the substrate polarization. In image charge theory, the metal electrons near a surface where a test charge or ion is present redistribute so that there is no electric field within the metal. This redistribution leads to an effective, or image, charge within the metal of opposite sign to the test charge at a distance below the image plane equal to the distance of the test charge above it; in this case, $Q = M_1/2$. This simple theory shows that the substrate polarization makes a large contribution to $M_1$ and explains the large $|M_1| > 1$ values in Table V.

In order to reduce this factor of 2 uncertainty in the estimate of the adsorbate $Q$, a further analysis of the dipole moment curves is required. One way to obtain additional information is to transform the $Ag_4X$ cluster orbitals into those which are most like X, denoted $\varphi_i(\text{loc,X})$, and the orthogonal complement of the SCF canonical space to the space of $\varphi_i(\text{loc,X})$. A corresponding orbital transformation[30,31] provides the required transformation to maximally localized orbitals. It has been performed between the $Ag_4X$ orbitals and the orbitals of the isolated X anion for a range of distances of X above the Ag surface. The contribution of the $\varphi_i(\text{loc,X})$ orbitals to the total cluster dipole is denoted $\mu(X)$ given by

$$\mu(X) = -\sum_i \langle \varphi_i(\text{loc,X})|z|\varphi_i(\text{loc,X})\rangle + Q_N Z_N\,, \tag{4}$$

where $Q_N$ and $Z_N$ are the charge and position above the surface, respectively, of the halogen nucleus. The Taylor expansion coefficients for $\mu(X;z)$ about $z_e$, Eq. (3), are given in Table V. The $\mu(X;z)$ curves are also linear but now the slope, $M_1$, provides more direct information about the halogen ionicity.

The $M_1(F) = -1.0$ (for both $Ag_4$ and $Ag_{10}$ clusters) and $M_1(Cl) \cong M_1(Br) = -1.1$ are fully consistent with the ionicity obtained from the projection of $Q_P \approx -1$. The $|M_1|$ for Cl and Br is larger than one because they have a modest polarizability; see $\alpha_D$ in Table II. The polarization of $X^-$ by $Ag_4^+$ is also reflected in the value of $M_0$ for $\mu(X)$. If the corresponding orbitals, $\varphi_i(\text{loc,X})$, were not polarized and were entirely of halogen character, the $M_0$ would equal $-z_e$. The presence of $Ag_4^+$ polarizes the $X^-$ charge toward the surface; $|M_0|$ is ~10% smaller than $z_e$ for F decreasing to $|M_0|$ being ~30% smaller than $z_e$ for the more polarizable Br. It remains only to directly examine the polarization effects for $Ag_4^+$; this is done in the following subsection.

Before closing this section, we compare, briefly, the results for $Ag_4F$ and $Ag_{10}F$ given in Table V. The dipole moments for $Ag_{10}F$ at $z_e$ and for bare $Ag_{10}$, $\mu(Ag_{10}) = 0.31$, give, using Eq. (2), a value for the F ionicity of $Q_D(Ag_{10}F) = 0.20$; this is similar to $Q_D(Ag_4F) = 0.09$. When the $\mu(X)$ for $Ag_{10}F$ and $Ag_4F$ are compared, the extremely similar values of $M_1$ give strong evidence for a F ionicity of $-1$ in both $Ag_4F$ and $Ag_{10}F$.

### C. Different bonding contributions to the interaction energy

A detailed method of analysis, the constrained space orbital variation (CSOV), has been developed to separately measure the importance of various charge rearrangements which occur when a bond is formed.[9,11,32] In particular, the CSOV method makes it possible to distinguish the consequences of intraunit charge polarization and interunit covalent and ionic bonding. Given the strong evidence, presented above, that the $Ag_4X$ binding is ionic, the starting point of

the CSOV analysis is taken as the unperturbed charge densities of the separated ionic units,[9] the $Ag_4^+$ cation and the $X^-$ anion. The anion is represented in two ways. First, by a unit point charge, PC = $-1$, placed at the position of the halogen nucleus; this models a spherical anion but neglects its spatial extent. For the second representation of the anion, the SCF orbitals of the isolated anion are superposed with the $Ag_4^+$ charge distribution; they are fixed and not allowed to change. However when the energy is evaluated, all interactions arising from the presence of the frozen X orbitals are taken into account, including the exchange interaction[32]; the spatial extent of the spherical $X^-$ anion is fully treated.

These two representations of the halogen anion are used for the first two steps of the CSOV process. In the first, the $Ag_4^+$ orbitals are fixed as they are obtained for isolated $Ag_4^+$; this wave function, denoted here as charge superposition of frozen orbital, is the starting point, or step 0, of the CSOV process.[11] The $Ag_4^+$ orbitals are also allowed to vary and change because of the presence of the X anion for both the PC and extended representations of $X^-$; this wave function, denoted $Ag_4^+$ variation or $V(Ag_4^+,Ag_4^+)$, is step 1 of the CSOV process. The $Ag_4^+$ variation takes the polarization of the $Ag_4^+$ by the presence of the anion into account. For each wave function, we report the interaction energy, defined such that $E_{INT} > 0$ corresponds to attraction, as the difference of the energy of $Ag_4X$ and the separated ionic subunits, $Ag_4^+$ and $X^-$; we also report the value of $\mu$. These results are given in Tables VI–VIII; in each case a distance of X above Ag close to $z_e$ is used.

We consider the results for $Ag_4X$. There is a large Coulomb attraction at the charge superposition step for both the PC and the extended $X^-$. Of course, the attraction for the PC will grow as it is moved closer to the surface; this does not occur for $X^-$ because of the repulsion arising from the nonbonding overlap of the $Ag_4^+$ and $X^-$ charge distributions (Pauli repulsion). For a wide range of distances about equilibrium, this repulsion varies exponentially; for $Ag_4F$ near $z_e$, the Pauli repulsion taken as the difference in $E_{INT}$ for the PC and for $F^-$ is 1.5 eV. We describe this as a surface "wall" effect. The overlap of the $Ag_4^+$ and $X^-$ charge distributions can also be seen in the difference of $\mu$ for the PC and $X^-$ cases at the charge superposition step. When the $Ag_4^+$ variation is permitted, there are large changes for $E_{INT}$ and $\mu$ both for the PC and $X^-$ cases. For $F^-$, the $\mu$ increases by $\sim 3$ a.u. because the $Ag_4^+$ electrons polarize by moving down or away from the negatively charged $F^-$. This large change in $\mu$ due to the Ag polarization explains the poor values of $Q_D$ obtained from Eq. (2), where this polarization is neglected. The $Ag_4^+$ polarization also increases $E_{INT}$ for $Ag_4F$ by $\sim 2.0$ eV. However, the surface wall remains, as can be seen by comparing the PC and $F^-$ values of $E_{INT}$ for the $Ag_4^+$ variation wave function. Similar conclusions are obtained from the $Ag_4Cl$ and $Ag_4Br$ results in Tables VII and VIII.

In addition to the charge superposition and $V(Ag_4^+,Ag_4^+)$ steps discussed above, the CSOV analysis contains four additional steps. Since these steps are used to measure the importance of changes which involve the halogen occupied and virtual orbitals, the approximation of treating the halogen anion as a point charge cannot be used.

In the next step of the CSOV process, step 2 or $V(Ag_4^+,$ all), the basis for the variation of the $Ag_4^+$ orbitals is extended to include the $X^-$ virtual orbitals; the $X^-$ occupied orbitals are still held fixed. This step indicates the amount of charge transfer from $Ag_4^+$ to $X^-$. It is important to note that basis set superposition can effect the result at this step[12] since the increased basis set for $Ag_4^+$ can improve the description of $Ag_4^+$ without any charge transfer or dative bonding taking place.

In CSOV step 3, the intra-unit polarization of $X^-$ due to

TABLE VI. CSOV analysis for $Ag_4F$ cluster at $z = 3.2$ a.u. (PC = point charge, see the text).[a]

| Step | | $E_{INT}/\Delta E_{INT}$ | $\mu/\Delta\mu$ |
|---|---|---|---|
| (0) Frozen orbital | PC | +4.82/· · · | −4.49/· · · |
| | $F^-$ | +3.37/· · · | −4.21/· · · |
| (1) $V(Ag_4^+,Ag_4^+)$ | PC | +6.92/+2.10 | −1.52/+2.97 |
| | $F^-$ | +5.25/+1.88 | −1.37/+2.84 |
| (2) $V(Ag_4^+,$all) | | +5.35/+0.10 | −1.43/−0.06 |
| (3) $V(F^-,F^-)$ | | +5.59/+0.24 | −1.15/+0.28 |
| (4) $V(F^-,$all) | | +5.84/+0.25 | −1.05/+0.10 |
| (5) $V$(cov) | | +5.85/+0.01 | −1.04/+0.01 |
| (6) Full SCF | | +5.88/+0.03 | −0.94/+0.10 |

[a] Interaction energies, $E_{INT}$, in eV are computed with respect to separate ions; $\mu$ in a.u.

TABLE VII. CSOV analysis for $Ag_4Cl$ cluster at $z = 4.3$ a.u. (PC = point charge, see the text).[a]

| Step | | $E_{INT}/\Delta E_{INT}$ | $\mu/\Delta\mu$ |
|---|---|---|---|
| (0) Frozen orbital | PC | +4.27/· · · | −5.59/· · · |
| | $Cl^-$ | +3.11/· · · | −5.29/· · · |
| (1) $V(Ag_4^+,Ag_4^+)$ | PC | +5.47/+1.20 | −3.03/+2.56 |
| | $Cl^-$ | +4.10/+0.99 | −2.90/+2.39 |
| (2) $V(Ag_4^+,$all) | | +4.16/+0.06 | −2.96/−0.06 |
| (3) $V(Cl^-,Cl^-)$ | | +4.54/+0.38 | −2.32/+0.64 |
| (4) $V(Cl^-,$all) | | +5.01/+0.47 | −2.05/+0.28 |
| (5) $V$(cov) | | +5.04/+0.03 | −2.00/+0.05 |
| (6)Full SCF | | +5.09/+0.06 | −1.64/+0.35 |

[a] Interaction energies, $E_{INT}$, in eV are computed with respect to separate ions; $\mu$ in a.u.

TABLE VIII. CSOV analysis for $Ag_4Br$ cluster at $z = 4.8$ a.u. (PC = point charge, see the text).[a]

| Step | | $E_{INT}/\Delta E_{INT}$ | $\mu/\Delta\mu$ |
|---|---|---|---|
| (0) Frozen orbital | PC | +4.04/· · · | −6.01/· · · |
| | $Br^-$ | +2.99/· · · | −5.93/· · · |
| (1) $V(Ag_4^+,Ag_4^+)$ | PC | +4.97/+0.93 | −3.73/+2.28 |
| | $Br^-$ | +3.76/+0.77 | −3.72/+2.21 |
| (2) $V(Ag_4^+,$all) | | +3.80/+0.03 | −3.76/−0.04 |
| (3) $V(Br^-,Br^-)$ | | +4.14/+0.35 | −3.10/+0.66 |
| (4) $V(Br^-,$all) | | +4.65/+0.50 | −2.65/+0.45 |
| (5) $V$(cov) | | +4.67/+0.02 | −2.58/+0.07 |
| (6) Full SCF | | +4.74/+0.07 | −2.21/+0.46 |

[a] Interaction energies, $E_{INT}$, in eV are computed with respect to separate ions; $\mu$ in a.u.

the presence of $Ag_4^+$ is taken into account. For this step, denoted $V(X^-,X^-)$, the $Ag_4^+$ orbitals are fixed as they were determined at the preceding step, $V(Ag_4^+,all)$. The $X^-$ orbitals are varied in the halogen anion virtual space; in effect, the halogen intraunit polarization due to the presence of the $Ag_4^+$ cluster cation is allowed. In the next CSOV step 4, $V(X^-,all)$, the space for the variation of the $X^-$ orbitals is increased to include the $Ag_4^+$ virtual orbitals; this step allows charge donation or covalent bonding to the $Ag_4^+$ virtual space. As for the $V(Ag_4^+,all)$ CSOV step 2, we must consider at this step, the possibility of BSSE artifacts.

In CSOV step 5, denoted $V(cov)$, the covalent mixing between the $V(X^-,all)$ step cluster valence $e$ orbitals, $(1e)^4$ $(X^-)$ and $(2e)^1$ $(Ag_4^+)$ is allowed; all other orbitals are fixed as determined in step 4. The result of step 5 is compared to the full unconstrained SCF result and if they are nearly the same this means that all important bonding contributions have been considered.

From Tables VI–VIII, it is apparent that the electrostatic interaction and the $Ag_4^+$ cluster polarization are by far the most important contributions to the bonding and that the other mechanisms do not change the interaction energy or dipole moment by large amounts. The change from $V(Ag_4^+,Ag_4^+)$ to $V(Ag_4^+,all)$ is small for all X; the increase in $D_e$ is $<0.1$ eV and the decrease in $\mu$ is $< -0.06$ a.u. If these changes are physical, they would require partial occupation of Rydberg orbitals of the closed shell halogen anion. It is extremely energetically unfavorable to add charge to $X^-$. Hence the small changes found at CSOV step 2 arise from BSSE. More significant is the energy lowering associated with the $X^-$ polarization, CSOV step 3 or $V(X^-,X^-)$, which, of course, is larger for the more polarizable Cl and Br atoms than for F. The polarization of $X^-$ toward the positive Ag surface leads to a positive change in $\mu$, $\Delta\mu$.

The full space variation of the $X^-$ charge in step 4 gives a 0.5 eV contribution to $E_{INT}$ for Cl and Br and a 0.25 eV contribution for F coming from the $X^-$ to $Ag_4^+$ charge transfer. These values must be considered as upper bounds because of the basis set superposition errors. The part of the contribution to $\Delta E$ at this CSOV step due to the basis set superposition errors can be estimated in the following way. The $\Delta E_{INT}$ at CSOV step 3, $V(X^-,X^-)$, which would arise if the $\alpha_D$ for the free anion were the BSSE value rather than the value for the isolated with halogen extended basis set is given by

$$\Delta E_{INT}(\text{CSOV step 3; BSSE corrected}) = \Delta E_{INT}(\text{CSOV step 3}) \times [\alpha_D(\text{BSSE})/\alpha_D(\text{extended basis})]. \quad (5)$$

The change in $\Delta E_{INT}$ is largest for Cl where it is 0.05 eV; for F and Br, the changes are 0.03 and 0.01 eV, respectively. This change should be used as an amount to reduce the $\Delta E_{INT}$ at CSOV step 4, $V(X^-,all)$, to account for the BSSE at this step. For Cl, this correction to the Cl back-donation contribution to the covalent bonding reduces the value from the directly calculated 0.47 to 0.42 eV. Clearly, the $V(X^-,all)$ CSOV results in Tables VI–VIII indicate a higher degree of covalency for the Ag–Cl and Ag–Br interactions than for the Ag–F interaction even when the BSSE effects are taken into account. This result is consistent with the projection operator analysis, Table IV.

As expected from the large $X^-$ ionicity, the $e^4$–$e^1$ covalent interaction at CSOV step 5 leads to very small changes in $E_{INT}$ and $\mu$. The near agreement between the full SCF and step 5 $E_{INT}$ shows that no important bonding effects have been neglected.

The CSOV analysis clearly shows that the electrostatic interaction and the cluster polarization alone account for about 80%–90% of the whole interaction energy. The main difference between F, Cl, and Br is that, because of the larger equilibrium bond distances, the electrostatic interaction and the Ag cluster polarization are smaller for Cl and Br than for F. On the other hand, the contribution from the Cl and Br polarization is higher, as expected on the basis of the larger dipole polarizabilities of these anions.

### D. Field effects on bond distances

A further proof of ionicity can be obtained by applying a uniform external electric field normal to the cluster surface. If the bonding is ionic, as shown by the previous analyses, the effect of the field would be that to move the negatively charged halogen up and down to an extent which depends on the sign and on the magnitude of the applied field.

The energies on the self-consistent field (SCF) potential surface for the variation of the $X^-$ geometry in the presence of the field are denoted $E_{SCF}(F,Z)$; $F$ is the magnitude of the electric field and $Z$ represents the ligand coordinate. The SCF variational solution is obtained with the Hamiltonian $H(F)$,

$$H(F) = H(0) + \mathbf{F}\cdot\sum_i \mathbf{r}_i - \mathbf{F}\cdot\sum_i \mathbf{R}_i, \quad (6)$$

where $H(0)$ is the usual $F=0$ Hamiltonian and $r_i$ $(R_i)$ are the electron (nuclear) coordinates. The first order perturbation theory energy, $E_P(F,Z)$, is defined[10,33] as the $F=0$ SCF energy, $E_{SCF}(0,Z)$, plus $\mu\times F$ where $\mu$ is the cluster dipole moment for the field free, $F=0$, case. The difference between $E_P(F,Z)$ and $E_{SCF}(0,Z)$ is a Stark effect[10,33]; it does not include any chemical change induced by the field. These electronic effects are explicitly considered in the SCF variational energy in the presence of the field, $E_{SCF}(F,Z)$. Hence, the differences between Stark and SCF values for the Ag–halogen bond distances are indicative of the importance of the chemical changes occurring in the bonding by effect of the external field. In the following we refer to the equilibrium bond distances for the $E_P(F,Z)$ potential curve as Stark values and to the full variational $E_{SCF}(F,Z)$ values simply as SCF.

The fields considered are $F=\pm 0.01$ a.u. $=\pm 5.7\times 10^7$ V/cm; this field is comparable to the fields at the electrode surface of an electrochemical cell when a potential of about 1 V is applied.[34] The sign convention is such that $F<0$ attracts electrons from the surface toward the ligand. Indeed, we observe large field-induced changes in equilibrium bond distance when $F=-0.01$ is applied. The $X^-$ ions are pulled away from the surface (Table IX) to equilibrium bond distances which are about 10% larger than

TABLE IX. Equilibrium bond distances in a.u. for halogens chemisorbed on $Ag_4$ in the presence of an external field $F$ (in a.u.). Both Stark and variational SCF values are given.

| $F$ | | $Ag_4F$ $z_e/\Delta z$ | $Ag_4Cl$ $z_e/\Delta z$ | $Ag_4Br$ $z_e/\Delta z$ |
|---|---|---|---|---|
| 0.00 | SCF | 3.310/··· | 4.347/··· | 4.721/··· |
| +0.01 | Stark | 3.098/−0.21 | 4.055/−0.29 | 4.405/−0.32 |
| | SCF | 3.092/−0.22 | 4.058/−0.29 | 4.418/−0.30 |
| −0.01 | Stark | 3.637/+0.33 | 4.893/+0.55 | 5.375/+0.65 |
| | SCF | 3.620/+0.31 | 4.904/+0.56 | 5.410/+0.69 |

for the $F = 0$ case. The ion shift follows the trend Br > Cl > F consistently with the sequence of dipole moments (Table III) and originates entirely from the interaction of the cluster dipole and the field (Stark effect). When the field $F = +0.01$ is applied, the ions are pushed toward the surface but the equilibrium distances vary to a smaller extent with respect to the $F = -0.01$ case because of the increasing Pauli repulsion ("wall effect") occurring when the $X^-$ ion approaches the cluster surface.

The very similar Stark and full variational SCF shifts in $z_e$ provide strong evidence that there are only small changes in the Ag–X bonding due to the presence of the electric field. The large field induced changes in $z_e$ are further evidence for the ionic character of the Ag–X bond.

## IV. F CHEMISORPTION ON OCTAHEDRAL SITE

The threefold site is known to be the preferred one for chemisorption of halogens on the Ag (111) surface.[1] However, it is experimentally difficult to distinguish between the tetrahedral and the octahedral sites of the Ag(111) surface. In the tetrahedral cavity, the presence of an Ag atom directly below the halogen adsorbate can in principle allow an easy electron redistribution (polarization) following the ion formation on the surface.

The two clusters chosen to model the octahedral site, $Ag_6$ and $Ag_7$, differ for the presence in the latter of an Ag atom in the third layer (Fig. 2). The results for F chemisorption on $Ag_6$ and $Ag_7$ are given in Table X. As found for $Ag_4F$ and $Ag_{10}F$ clusters, also the $Ag_6$ and $Ag_7$ clusters exhibit close values for bond distances (the difference is about 1%), similar but not identical vibrational frequencies (here the difference is around 7%), but dramatically different values of the binding energies (about 0.8 eV difference for the dissociation into $F^-$ and $Ag_n^+$, Table X). However, despite these

TABLE X. Chemisorption properties for F atom on $Ag_6$ and $Ag_7$ clusters.[a]

| Cluster | | $Ag_6F$ | $Ag_7F$ |
|---|---|---|---|
| Bare $Ag_n$ clusters | | | |
| IP | (eV) | 5.54 | 4.31 |
| $\mu(Ag_n)$ | (a.u.) | 0.06 | −0.26 |
| $\mu(Ag_n^+)$ | (a.u.) | −2.10 | −3.09 |
| $Ag_6F$ and $Ag_7F$ clusters | | | |
| $z_e$ | (a.u.) | 3.333 | 3.291 |
| $\omega_e$ | ($cm^{-1}$) | 252 | 273 |
| $D_e(Ag_n + X)$ | (eV) | 0.44 | 2.48 |
| $D_e(Ag_n^+ + X^-)$ | (eV) | 4.60 | 5.41 |
| $Q_P$ | | −0.98 | −0.98 |
| $\mu(Ag_nF)$ | $M_0$ | −0.02 | −1.16 |
| | $M_1$ | −1.05 | −1.53 |
| | $M_2$ | −0.41 | −0.15 |
| | $M_3$ | +0.09 | +0.04 |
| $\mu(F^-)$ | $M_0$ | −3.04 | −3.00 |
| | $M_1$ | −0.99 | −0.96 |
| | $M_2$ | −0.05 | −0.04 |
| | $M_3$ | +0.00 | −0.01 |

[a] The three surface Ag atoms are treated with a 11 electron ECP; the remaining Ag atoms are treated with a 1 electron ECP.

different binding energies for $Ag_6X$ and $Ag_7X$, the nature of Ag–halogen interaction is the same for both clusters. The projection and the dipole moment analysis, Table X, indicate that the bonding is ionic and that $F^-$ is formed; this is the same bonding found for the tetrahedral site with the $Ag_4F$ and $Ag_{10}F$ clusters.

In order to better understand the bonding mechanism in $Ag_6F$ and $Ag_7F$, and therefore to rationalize the observed differences in binding energies, we performed a CSOV analysis. This analysis has been carried out in a somewhat different fashion than the more conventional CSOV analysis for the $Ag_4X$ clusters described in Sec. III C. The different approach is taken because our primary concern is to understand the origin of the different $D_e$ for the $Ag_6F$ and $Ag_7F$ clusters. The $E_{INT}$ defined, as before, with respect to the energies of the $Ag_n^+$ and $F^-$ ions and the $\mu$ are given in Table XI. The CSOV is started by placing a point charge, PC = −1, at $z = 3.2$ a.u. above $Ag_n^+$; this distance is near $z_e$ for both $Ag_6F$ and $Ag_7F$, see Table X. The $E_{INT}$ for the electrostatic interaction of the fixed SCF orbitals of $Ag_n^+$ with PC, denoted FO $Ag_n^+$-PC, is 1.5 eV larger for the $Ag_7$ than for the $Ag_6$ cluster. This difference must arise from the different 5*sp* "conduction" band charge distribution for the two clusters. Still representing the F anion by the PC, the

TABLE XI. CSOV analysis for $Ag_6F$ and $Ag_7F$ clusters at $z = 3.2$ a.u. (PC = point charge, see text).[a]

| Step | $Ag_6F$ $E_{INT}/\Delta E_{INT}$ | $Ag_6F$ $\mu/\Delta\mu$ | $Ag_7F$ $E_{INT}/\Delta E_{INT}$ | $Ag_7F$ $\mu/\Delta\mu$ |
|---|---|---|---|---|
| FO $Ag_n^+$ − PC | +2.56/··· | −5.30/··· | +3.99/··· | −6.29/··· |
| Pol. $Ag_n^+$ − PC | +5.72/··· | +0.04/··· | +6.52/··· | −1.54/··· |
| Pol. $Ag_n^+$ − PC/F | +3.77/−1.95 | +0.24/+0.20 | +4.65/−1.87 | −1.37/+0.17 |
| $V(Ag_4^+,all)$ | +3.90/+0.13 | −0.14/−0.38 | +4.74/+0.09 | −1.40/−0.03 |
| $V(F^-,all)$ | +4.55/+0.65 | +0.13/+0.27 | +5.39/+0.64 | −1.12/+0.28 |
| Full SCF | +4.60/+0.05 | +0.11/−0.02 | +5.41/+0.02 | −1.13/+0.09 |

[a] Interaction energies, $E_{INT}$, in eV are computed with respect to separate ions; $\mu$ in a.u.

$Ag_n^+$ charge distribution is allowed to polarize in response to the presence to the presence of the PC; this step is denoted Pol $Ag_n^+$-PC. The $Ag_6^+$ polarization increases $E_{INT}$ by 3.2 eV while that for $Ag_7^+$ is increased by 0.7 eV less or 2.5 eV. The larger polarization of the $Ag_6^+$ cluster leads to an increase of $\mu$ by 5.3 a.u. while the increase due to the $Ag_7^+$ polarization is smaller, 4.8 a.u. The difference in $E_{INT}$ for $Ag_6^+$ and $Ag_7^+$ at Pol. $Ag_n^+$-PC of 0.8 eV is almost the same difference found at the Full SCF level for $Ag_6F$ and $Ag_7F$. The differences arises from canceling FO electrostatic contributions due to the distribution of conduction band charge, favoring $D_e$ for $Ag_7^+$, and the $Ag_n^+$ polarization, favoring $D_e$ for $Ag_6^+$.

At this point, the $Ag_n^+$ charge distribution is fixed and the PC is replaced by the fixed, frozen, charge distribution for extended $F^-$ anion; this step is denoted Pol. $Ag_n^+$-PC/$F^-$. The Pauli repulsion arising from the nonbonding overlap of $Ag_n^+$ and $F^-$ charge distributions is large, $\sim 2$ eV, but is the same for $Ag_6F$ and $Ag_7F$ within 0.1 eV. The following CSOV steps, $V(Ag_n^+,\text{all})$ and $V(F^-,\text{all})$ take account of the full basis set rearrangements of $Ag_n^+$ and $F^-$, respectively. The changes in $E_{INT}$ at these steps are very similar for $Ag_6F$ and $Ag_7F$. Further, the results at $V(F^-,\text{all})$ are close to the Full SCF values for both $E_{INT}$ and $\mu$.

These CSOV show that while the nature of the bonding between clusters and adsorbates is basically independent of cluster shape and nuclearity, the precise values for the chemisorption properties, especially for the $D_e$, are very cluster dependent. This rules out the possiblity to distinguish, on the basis of the present cluster calculations, whether the tetrahedral or the octahedral is the preferred site for halogen chemisorption on Ag (111) surfaces.

## V. CONCLUSIONS

The various methods that have been used to characterize the Ag–halogen bond provide consistent evidence that the bond is essentially entirely ionic. They show that a commonly used measure of ionicity obtained from the change in the work function or dipole moment is incorrect because it neglects the metal polarization. The comparison of the interaction of $Ag_4^+$ with a point charge and with the extended halogen anion shows that there is a large Pauli repulsion opposing the Coulomb attraction and describable as a surface wall. There is also a large contribution arising from the polarization of the surface charge which is commonly described as an "image charge" effect.[29] This surface polarization contributes a large amount not only to the interaction energy but also to the dipole moment. It explains why the work function does not provide a proper measure of the bond ionicity.[9] The contributions arising from the anion polarizaton and from the covalent Ag-halogen bonding are much smaller.

## ACKNOWLEDGMENTS

One of us (G.P.) is grateful to IBM Italy for partially supporting his stay at the IBM Alamden Research Center. This work has been supported, in part, by the Office of Naval Research.

[1] G. M. Lamble, R. S. Brooks, S. Ferrer, D. A. King, and D. Norman, Phys. Rev. B **34**, 2975 (1986).
[2] J. G. Gordon II, M. Samant, and O. Melroy (private communication).
[3] M. Deakin, T. Li, and O. Melroy, J. Electroanal. Chem. **243**, 343 (1988).
[4] D. M. Kolb, Z. Phys. Chem. **154**, 179 (1987).
[5] D. Larkin, K. L. Guyer, J. T. Hupp, and M. J. Weaver, J. Electroanal. Chem. **138**, 401 (1982).
[6] J. W. Schultze and F. D. Koppitz, Electrochim. Acta **21**, 327 (1976).
[7] J. W. Schultze and K. J. Vetter, J. Electroanal. Chem. **44**, 63 (1973).
[8] C. J. Nelin, P. S. Bagus, and M. R. Philpott, J. Chem. Phys. **87**, 2170 (1987).
[9] L. G. M. Pettersson and P. S. Bagus, Phy. Rev. Lett. **56**, 500 (1986).
[10] P. S. Bagus, C. J. Nelin, W. Muller, M. R. Philpott, and H. Seki, Phys. Rev. Lett. **58**, 59 (1987).
[11] P. S. Bagus, K. Hermann, and C. W. Bauschlicher, J. Chem. Phys. **81**, 1966 (1984).
[12] P. S. Bagus, C. J. Nelin, and C. W. Bauschlicher, Phys. Rev. B **28**, 5423 (1983).
[13] P. J. Hay and W. R. Wadt, J. Chem. Phys. **82**, 299 (1985).
[14] P. J. Hay and W. R. Wadt, J. Chem. Phys. **82**, 270 (1985).
[15] P. J. Hay and R. L. Martin, J. Chem. Phys. **83**, 5174 (1985).
[16] F. B. van Duijeneveldt, IBM Res. Rep. No. RJ945 (1971) (unpublished).
[17] B. Roos and P. Siegbahn, Theoret. Chim. Acta **17**, 209 (1970).
[18] (a) S. Huzinaga, J. Chem. Phys. **66**, 4245 (1977); (b) S. Huzinaga, J. Andzelm, M. Klobukowski, E. Radzio-Andzelm, A. Sakai, and H. Tatewaki, *Gaussian Basis Sets for Molecular Calculations* (Elsevier, Amsterdam, 1984).
[19] E. Clementi and C. Roetti, At. Data Nucl. Data Tables **14**, 177 (1974).
[20] S. Fraga, K. M. Saxena, and B. W. N. Lo, At. Data Nucl. Data Tables **3**, 323 (1971).
[21] H. Hotop and W. C. Lineberger, J. Phys. Chem. Ref. Data **4**, 539 (1975).
[22] F. Sasaki and M. Yoshimine, Phys. Rev. A **9**, 26 (1974).
[23] J. O. Hirschfelder, C. F. Curtiss, and R. B. Bird, *Molecular Theory of Gases and Liquids* (Wiley, New York, 1964).
[24] G. Herzberg, *Infrared and Raman Spectra of Polyatomic Molecules* (Van Nostrand, New York, 1945).
[25] P. S. Bagus, C. J. Nelin, and C. W. Bauschlicher, J. Chem. Phys. **79**, 2975 (1983).
[26] K. Hermann, P. S. Bagus, and C. J. Nelin, Phys. Rev. B **35**, 9467 (1987).
[27] T. A. Delckar, F. C. Tompkins, and F. S. Ham, Proc. R. Soc. London Ser. A **300**, 141 (1967).
[28] D. Westphal and A. Goldmann, Surf. Sci. B **1**, 113 (1983).
[29] N. D. Lang, Surf. Sci. **127**, L118 (1983).
[30] A. T. Amos and G. G. Hall, Proc. R. Soc. London Ser. A **263**, 483 (1961).
[31] M. Seel and P. S. Bagus, Phys. Rev. B **28**, 2023 (1983).
[32] P. S. Bagus, K. Hermann, and C. W. Bauschlicher, J. Chem. Phys. **80**, 4378 (1984).
[33] P. S. Bagus, C. J. Nelin, K. Hermann, and M. R. Philpott, Phys. Rev. B **36**, 8169 (1987).
[34] J. O. M. Bockris and A. K. N. Reddy, *Modern Electrochemistry* (Plenum, New York, 1973), Vol. 2.